PERGAMON

Journal of Geodynamics 33 (2002) 269–280

JOURNAL OF
GEODYNAMICS

www.elsevier.com/locate/jgeodyn

Oceanic and soil moisture contributions to seasonal polar motion

J. Wünsch*

GeoForschungsZentrum Potsdam, Division Kinematics and Dynamics of the Earth, Telegrafenberg, D-14473 Potsdam, Germany

Received 8 June 2001; accepted 27 September 2001

Abstract

Oceanic contributions to the annual and semi-annual wobble of polar motion have been evaluated by Wünsch (Wünsch, J., 2000. Oceanic influence on the annual polar motion. J. Geodynamics 30, 389–399) using three different ocean circulation models: (a) the Parallel Ocean Climate Model (Semtner, A.J., Chervin, R.M., 1992. Ocean circulation from a global eddy-resolving model. J. Geophys. Res. 97, C4, 5493–5550; (b) the model used by Ponte et al. (Ponte, R.M., Stammer, D., Marshall, J., 1998. Oceanic signals in observed motions of the Earth's pole of rotation. Nature 391, 476–479); (c) the Hamburg Ocean Model for Circulation and Tides used by Thomas and Sündermann [Thomas, M., Sündermann, J., 1998. Zur simultanen Modellierung von allgemeiner Zirkulation und Gezeiten im Ozean und Auswirkungen auf bestimmte Erdrotations parameter. In: Freeden, W. (Ed.), Progress in Geodetic Science. Aachen, pp. 144–151]. That result is extended by considering oceanic refinements as well as time variable soil moisture and snow load. Five soil moisture models were used. The snow load according to Chao et al. (Chao, B.F., O'Connor, W.P., Chang, A.T.C., Hall, D.K.,Foster, J.L., 1987. Snow-load effect on the Earth's rotation andgravitational field 1979-1985. J. Geophys. Res. 92, 9415–9422) was added to this in an attempt to close the balance. The NCEP/NCAR reanalysis atmosphere + Ponte et al. (1998) ocean + Chao and O'Connor (Chao, B. F., O'Connor, W. P., 1988. Global surface-water-inducedseasonal variations in the Earth's rotation and gravitational-field. Geophys. J. 94, 263–270) (rain + snow) nearly close the annual balance of polar motion excitation, i.e. it is very close to the geodetic excitation functioncomputed from the time series of the IERS (International Earth Rotation Service). The other models of soil moisture differ in theirpolar motion contribution from the Chao and O'Connor (1988) estimates. Further improvements in this work await results from the space gravity missions CHAMP, GRACE and GOCE.

* Corresponding author. Tel.: +49-331-288-1149; fax: +49-331-288-1163.
E-mail address: wuen@gfz-potsdam.de (J. Wünsch).

0264-3707/02/$ - see front matter
PII: S0264-3707(01)00070-9

1. Introduction and motivation

The polar motion of the Earth consists mainly of ellipses centered on the origin of coordinates with periods of 1.00 a, 0.50 a and the Chandler period of about 435 days = 1.19 a. It is generally recognized that the Chandler period represents an eigenmode of the Earth, whereas the annual and semi-annual periods are forced by seasonal redistribution of mass and motions within the Earth system.

King and Agnew (1991) described the annual wobble by plotting vectorsums of the contributions (atmosphere, soil moisture, ocean) then available. Ponte and Stammer (1999) presented a work similar to Wünsch (2000) (henceforth W2000), where they gave phasor diagrams for polar motion at annual, semi-annual and Chandler periods. They also discussed thoroughly the ocean model they used. Based on the ocean circulation model POCM_4B, Johnson et al. (1999) presented oceanic angular momentum (OAM) on interannual to submonthly timescales. They published phasor plots at the annual, semi-annual and biennial period. Chen et al. (2000) used hydrological (NCEP/NCAR reanalysis soil moisture and snow) and oceanic data (TOPEX/POSEIDON altimetry) to derive time series of excitation functions which they compared with observations. Abarca del Rio (1997) and Dill (2001) also employed soil moisture models for investigations of polar motion. Robock et al. (1998) described an intercomparison of many soil moisture models used for meteorological purposes (Atmospheric Model Intercomparison Project). The steadily growing number of soil moisture measurements is discussed by Robock et al. (2000).

In this work, we concentrate mainly on the annual and semi-annual periods and sum up their possible causes, i.e. atmosphere + oceans + variable soil moisture. The presented ellipses are tabulated for the **ocean models** and for five models of **variable soil moisture**. Wünsch (2000) had consideredocean + atmosphere, while here soil moisture and snow load are also considered. This addition is expected to nearly close the annual excitation budget and explain the causes of annual polar motion. Soil moisture variations are part of the global water cycle. The ellipse quantities are compared to residuals, i.e. excitation from observations (IERS)—the atmospheric part from NCEP/NCAR reanalysis. (NCEP = National Centers for Environmental Prediction; NCAR = National Center for Atmospheric Research).

The five models of soil moisture mentioned are the following: Huang et al. (1996) calculated soil moisture using a water balance equation including precipitation, evaporation, runoff and groundwater loss. Model parameters were estimated using observed precipitation, temperature and runoff from Oklahoma between 1960 and 1989. Comparing the modelled values with 8 years (1984–1991) of soil moisture observed in Illinois indicated the model gave a reasonable simulation of soil moisture content including both climatology and interannual variability. Chao and O'Connor (1988) modelled the seasonal cycle in continental surface water storage using a global meteorological data set of precipitation (snow and rain) and evapotranspiration. Kuehne and Wilson (1991) estimated water storage variations within 612 river drainage basins from measurements of precipitation and temperature. Their water storage includes snow load. The NCEP/NCAR Climate Data Assimilation System I (CDAS-1) soil moisture data are described by Kalnay et al. (1996). A calculation according to the proposal by Kikuchi (1977) was done by the present author, see Section 5.1.

2. Basic formulae

Free rotational motions of a deformable Earth are governed by the linearized Liouville equations (W2000). Let us summarize some equations used in the following.

Traditionally, polar motion (i.e. the orientation of the rotation axis within the solid Earth) is described by its x and y components, where y is defined to be positive towards 90°W longitude. This is a left-handed coordinate system. x and y are expressed, for example, in seconds of arc. We also use a right handed system p_1, p_2, where the observable polar motion $p(t) = p_1(t) + i \cdot p_2(t) = x(t) - i \cdot y(t)$ of the Celestial Ephemeris Pole CEP (complex notation, $i = \sqrt{-1}$). This is described by the linearized Liouville equations (Munk and MacDonald 1960):

$$p(t) + \frac{i}{\sigma_0}\dot{p}(t) = \chi(t). \tag{1}$$

The usage of complex quantities is equivalent to two-dimensional vectors. Here σ_0 is the (complex) angular velocity corresponding to the observed Chandler mode with a period $P = 1.19$ a and quality factor $Q = 50$ (Jochmann, 1999). Geophysical information is contained in the right-hand-side term $\chi(t)$. The dimensionless complex χ-function (called equatorial effective angular momentum function EAMF) is defined as (Wahr, 1982; Barnes et al., 1983; Gross, 1993):

$$\chi(t) = \chi_1 + i \cdot \chi_2 = 1.61 \cdot [\Omega \Delta I(t)/1.44 + \Delta h(t)]/[\Omega(C - A)] \tag{2}$$

where $\Omega = 7.292115 \cdot 10^{-5}$ s^{-1}, (mean angular velocity of rotation of the Earth) and $C = I_3$, $A = I_1$ are the principal moments of inertia of the Earth. The term with the inertia tensor components $\Delta I(t)$ is the matter term (or mass term), whereas the term with the relative angular momentum $\Delta h(t)$ is the motion term:

$$\Delta I = \Delta I_{13} + i \cdot \Delta I_{23}, \Delta h = \Delta h_1 + i \cdot \Delta h_2 \tag{3}$$

In earlier literature, the excitation function ψ is often used (Munk and MacDonald, 1960; Lambeck, 1980), which is defined as:

$$\psi(t) = \chi(t) - \frac{i}{\Omega}\frac{\mathrm{d}}{\mathrm{d}t}\chi(t). \tag{4}$$

which contains terms in $\Delta\dot{I}$ and $\Delta\dot{h}$. Gross (1992) showed that χ (and not ψ) should be inserted into the right-hand sides of the Liouville equations because of the nature of the measured polar motion. However, the distinction between χ and ψ is only relevant for short period motions, such as diurnal and subdiurnal tidal periods. In the case of annual periods of interest here, this distinction can be neglected.

The equatorial excitation function components χ_1 and χ_2 occurring on the right-hand side of the Liouville equations describe an ellipse (Munk and MacDonald, 1960) as the superposition of prograde and retrograde circular components. For example, for the atmosphere, in the case of a single frequency (annual or semi-annual), χ may be expressed as:

$$\chi = (A_+ + i \cdot B_+)e^{i\omega t} + (A_- + i \cdot B_-)\mathrm{e}^{-i\omega t} \tag{5}$$

where A_+ and B_+ are the real and imaginary parts of the prograde amplitude and A_- and B_- are the real and imaginary parts of the retrograde amplitude. The geometrical ellipse parameters are:

semi-major axis a, semi-minor axis b and inclination angle γ of the semi-major axis with respect to the x-axis. In the tables presented, β is the phase angle when the tip of the ellipse is reached, counted from the beginning of the year. From Eq. (5), it is clear that the sum or difference of two ellipses with the same angular frequency ω is again an ellipse centered at the origin, for example atmosphere + ocean.

Four independent ellipse parameters A_+, B_+, A_- and B_- are determined from the model data by two-dimensional Fourier analysis (Jochmann, 1993; Jochmann and Felsmann, 2001). This Fourier method includes a correction for the non-orthogonality of the trigonometric functions over a finite interval of time.

3. Remarks on the atmosphere and the ocean

Table 1 is mostly repeated from W2000, except for the entries in bold: 'AAM JMA', 'IERS–JMA', 'OMCT (IB)' and 'OMCT IB matter'. Most of the derived excitation ellipses in the following tables are very narrow, i.e. the semi-minor axis b is very small. 'χ from IERS' means excitation functions χ computed from a very accurate observed polar motion time series compiled by IERS (series C04, cf. IERS, 1997). This series is based on space geodetic measurements for the time interval used (1986–1997). 'AAM NCEP smooth' is the ellipse caused by atmospheric pressure and wind, as given byNCEP/NCAR reanalysis (Kalnay et al., 1996; Salstein and Rosen, 1997).

Table 1
Comparison of annual ellipses of the excitation function $\chi = \chi_1 + i \cdot \chi_2$ of polar motion; units are ma s; γ and β are in degrees[a]

Description	A_+	B_+	A_-	B_-	σ_A	a	b	γ	β
Ellipses									
χ From IERS	5.89	−11.61	−1.92	−4.44		17.9	8.18	91.8	154.9
AAM NCEP smooth	−0.86	−16.57	−2.36	−14.10	±0.66	30.9	2.29	83.8	176.7
AAM JMA	1.26	−13.81	−3.19	−9.04		23.3	4.16	82.9	167.7
Differences									
IERS–NCEP	6.75	4.96	0.44	9.66		18.1	−1.29	61.9	25.5
IERS–JMA	4.63	2.20	1.27	4.60		9.9	0.35	50.0	24.6
Höpfner (1996)	8.86	1.85	0.09	9.97		19.0	−0.92	50.6	38.8
Lageos-(Chao and Au, 1991)	9.27	1.65	0.57	8.53		18.0	0.87	48.1	38.0
Ocean models									
POCM (CSR)	0.95	1.12	0.43	2.50	±0.94	4.0	−1.06	65.0	15.3
Wahr (1983)	0.16	−1.44	1.00	1.64		3.4	−0.47	167.5	251.1
Ponte et al., (1998)	5.35	4.18	−2.41	6.39	±1.26	13.6	−0.04	74.3	36.4
OMCT (1998)	12.01	0.89	14.53	19.15	±1.44	36.1	−12.01	28.5	24.3
OMCT (IB)	6.09	−6.04	1.67	10.35	±0.70	19.1	−1.91	18.1	62.8
OMCT IB matter	8.18	−4.13	1.36	8.60	±0.52	17.9	0.46	27.1	53.9

[a] A_+ and B_+ are the real and imaginary parts of the prograde amplitude; A_- and B_- are those of the retrograde amplitude. σ_A is the standard deviation of the amplitudes A_+, B_+, A_- and B_-. Ellipse parameters are (Munk and MacDonald 1960): semi-major axis a, semi-minor axis b and inclination angle γ of the semi-major axis with respect to the x-axis. β is the phase angle when the apex of the ellipse is reached, counted from the beginning of the year.

'Smooth' means an averaging of the AAM values at 0, 6, 12 and 18 h in order to avoid diurnal variations. The Inverted Barometer for the pressure term (matter term) χ^p was used. The atmosphere is the biggest contributor to the annual polar motion (Chao and Au, 1991; W2000).

'AAM JMA' refers to the Atmospheric Angular Momentum determined by the Japan Meteorological Agency, see Aoyama and Naito (2000), who gave the annual χ_1, χ_2 in their Table 2a, under the entry 'IB-Pressure + Wind, JMA[SP]'. Here, SP is the so-called surface pressure method of calculating AAM. Their AAM JMA data were from 1 March 1988, to December 31 1997. This is nearly the same time interval as the entries 'AAM NCEP smooth' and 'χ from IERS, (1986–1997), selected to minimize the influence of interannual variations in the ellipse parameters a, b, γ and β. Note that the difference ellipse 'IERS–JMA' has a very small semi-major axis a of 9.9 ma s. Further difference ellipses are taken from Höpfner (1996) and Chao and Au (1991) 'Lageos-(Chao and Au)'.

The ocean is also a significant contributor to the seasonal polar motion. Table 1 contains results from Wahr (1983) and from Johnson et al. (1999) using the model POCM_4B (Semtner and Chervin, 1992; Stammer et al., 1996). Ocean results for $\chi_1(t)$, $\chi_2(t)$ from Ponte et al. (1998) were also studied. Both the POCM_4B and the model used by Ponte et al. (1998) are described in W2000. 'OMCT' (Ocean Model for Circulation and Tides) is the ocean circulation model of the Institut fur Meereskunde, University of Hamburg (cf. Section 3.). In addition, compared to the tables in W2000, 'OMCT IB' refers to 'Inverted Barometer': the ocean surface is not rigid, but reacts to the atmospheric pressure loading. In order to take this into account, the air pressure is kept constant over the model ocean ($p_a = 0$ over ocean). OMCT IB results for OAM were used from January 1975 to December 1984. Clearly, the IB assumption has a strong impact on the results, compared to the previous model run ['OMCT (1998)', cf. W2000]. 'OMCT IB matter' is only the matter part of the above (i.e. tensor of inertia changes), which dominates over the motion part. The OMCT IB semi-major axis of excitation ellipse (19.1 ma s) is comparable to the Ponte et al. (1998) result (13.6 ma s). However, the ellipse orientation angles γ do not agree well, being 18° and 74° for this work and Ponte et al. (1998), respectively.

Table 2
Annual excitation functions of soil moisture models[a]

Description	A_+	B_+	A_-	B_-	a	b	γ	β
Soil moisture								
Huang et al. 1996 soil moisture	5.88	−0.39	−6.09	0.77	12.01	−0.24	84.5	88.3
Chao and O'Conner, 1988 rain	2.12	2.77	−1.31	3.90	7.6	−0.63	80.6	28.0
Kuehne and Wilson 1991 'WATER'	1.65	−0.69	−6.82	0.59	8.6	−5.1	76.2	98.9
Reanalysis soil moisture	−3.30	−10.33	6.70	−5.24	19.3	2.33	107.1	214.8
Kikuchi calculation	2.99	−0.44	−4.35	1.20	7.5	−1.49	78.1	86.4
Chao et al., 1987 snow	−1.6	−4.6	4.2	−2.3	9.7	0.08	111.1	220.2
Chao and O'Conner, 1988 sum	0.52	−1.83	2.89	1.60	5.2	−1.40	157.4	231.6

[a] Chao and O'Connor (1988): 'rain' = soil moisture; sum = rain + snow. 'Reanalysis soil moisture' = model soil moisture from NCEP/NCAR reanalysis (CDAS-1) (Kalnay et al. 1996), excluding Antarctica. Units are [milliarcseconds]. 20.626 ma s = $1{\cdot}10^{-7}$ rad.

4. The ocean circulation model OMCT

The Hamburg ocean model OMCT (Thomas and Sündermann, 1998, 2000; Thomaset al., 2001) is based on the nonlinear equations of conservation of momentum, the equation of continuity of an incompressible fluid, and the equations of conservation of heat and salinity. Both the hydrostatic and the Boussinesq approximation are used. Sea ice is modelled in a manner similar to that of Hibler (1979). OMCT has 13 layers with a grid of $1.875\times1.875^\circ$ and a time step of 1 h. At the sea surface, OMCT is driven by wind stress, temperature and fresh water fields derived from the atmospheric model ECHAM3-T21. The IB version of OMCT in Table 1 is comparable to the excitation ellipse produced by the model used by Ponte et al. (1998) (MIT model). OMCT was also used by Wünsch et al. (2001) to study oceanic bottom pressure variations.

5. Annual excitation functions of soil moisture and snow load

Table 2 lists numerical values for the soil moisture contribution to annual polar motion derived using five different hydrological models. These contributions are relatively small, with the semi-major axis a around 8 ma s, except for the NCEP/NCAR reanalysis soil moisture data set which gave 19.3 ma s.

The Huang et al. (1996) soil moisture data ($1\times1^\circ$ grid) were used for the time interval from January 1968 to December 1978. The Stokes coefficients $\bar{C}_{21}(t)$, $\bar{S}_{21}(t)$ were obtained as surface integrals over the Earth's surface. As detailed in W2000, a conversion factor then leads to the matter terms of $\chi_1(t)$, $\chi_2(t)$. Fig. 1 shows monthly values of HAM (hydrological angular momentum) for these data.

The NCEP/NCAR Climate Data Assimilation System I (CDAS-1) soil moisture data were used for the interval January 1995 to December 1996 (24 months). The contributions from two soil levels were added with Antarctica excluded. As with the Huang et al. (1996) data, the computed Stokes coefficients $\bar{C}_{21}(t)$, $\bar{S}_{21}(t)$ led to the matter terms of HAM. A least-squares fit over the 24 months gave annual and semi-annual amplitudes χ_1^c, χ_1^s, χ_2^c, χ_2^s of the $\cos\omega t$ and $\sin\omega t$ components, from which the excitation function ellipses were calculated. The table entries for Chao and O'Connor (1988) and Kuehne and Wilson (1991) are from the respective publications.

While the Huang et al. (1996), Chao and O'Connor (1988) rain contribution, Kuehne and Wilson (1991), NCEP/NCAR reanalysis soil moisture results and the Kikuchi calculation (see Section 5.1.) do not fully agree with each other in the coefficients A_+, B_+, A_, B_-,there is some quite encouraging agreement in the ellipse parameters semi-major axis a and orientation angle γ, i.e. in the shapes of the ellipses. The angle β is around 90° in three cases.

Figs. 2 and 3 illustrate the resultant excitation functions. On the planes of coefficients (A_+, B_+) and (A_-, B_-), there is some similarity between the models Huang et al. (1996), Kuehne and Wilson (1991) and the Kikuchi calculation, i.e. the quadrants agree. The Kuehne and Wilson (1991) model has a large retrograde contribution, i.e. large A_- and B_- values compared to smaller prograde A_+ and B_+ parts.

The NCEP/NCAR reanalysis soil moisture gives a very big semi-major axis a, a fact which was also found in the time series of Chen et al. (2000).

In Table 2, 'Chao et al. 87 snow' is the snow load contribution to polar motion according to Chao et al. (1987), as repeated in Chao and O'Connor (1988). The value 'Chao and O'Connor

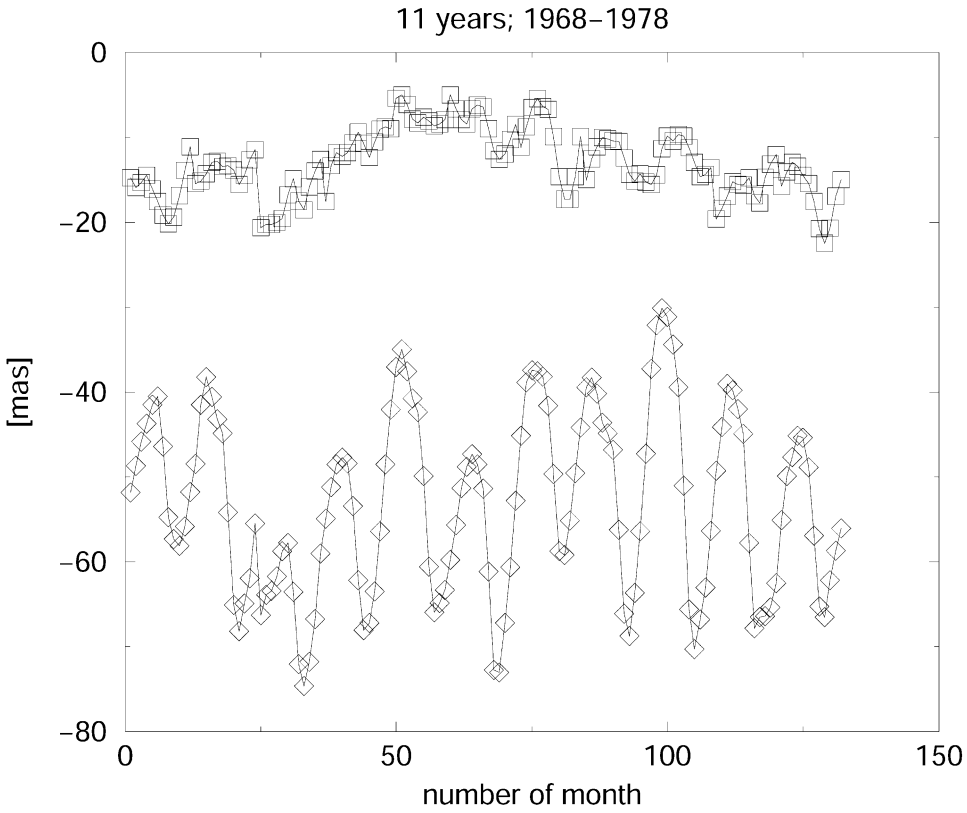

Fig. 1. Excitation function $\chi_1(t)$ (upper curve) and $\chi_2(t)$ (lower curve) caused by variable soil moisture according to the model of Huang et al. (1996) for monthly time steps.

1988 sum' shows a partial cancelation in the semi-major axis a values from the soil moisture (called 'rain') and snow load.

5.1. A Kikuchi calculation for soil moisture

The line 'Kikuchi calculation' in Table 2 is derived as follows (Kikuchi, 1977; Jochmann, 1999): the following approximate equation is used to calculate soil moisture Δs_j of month number j from the precipitation P_j of month j and the soil moisture $\Delta s_{(j-1)}$ of the previous month (j–1) at each block (compartment) on the continents:

$$\Delta s_j = k \cdot P_j + l \cdot \Delta s_{(j-1)} \tag{6}$$

where k and l are coefficients that are assumed as constants: $k = 0.50$, $l = 0.87$ as in Jochmann, (1999).

Exceptions are for blocks when the temperature $T < 0\ ^\circ$C, in which case $k = 1.00$, indicating snow on the ground. For the Kikuchi calculation, monthly GPCP (Global Precipitation Climatology Project) precipitation data on a $2.5 \times 2.5^\circ$ grid served as 'input' for January 1988 to December 1994. The soil moisture field for the starting epoch (December 1987) was taken from the NCEP/NCAR reanalysis soil moisture fields (the sum of two soil levels). The final polar motion ellipse was obtained from a least-squares fit to $\chi_1(t)$, $\chi_2(t)$ of the model years 1993 + 1994 ($n = 24$ months).

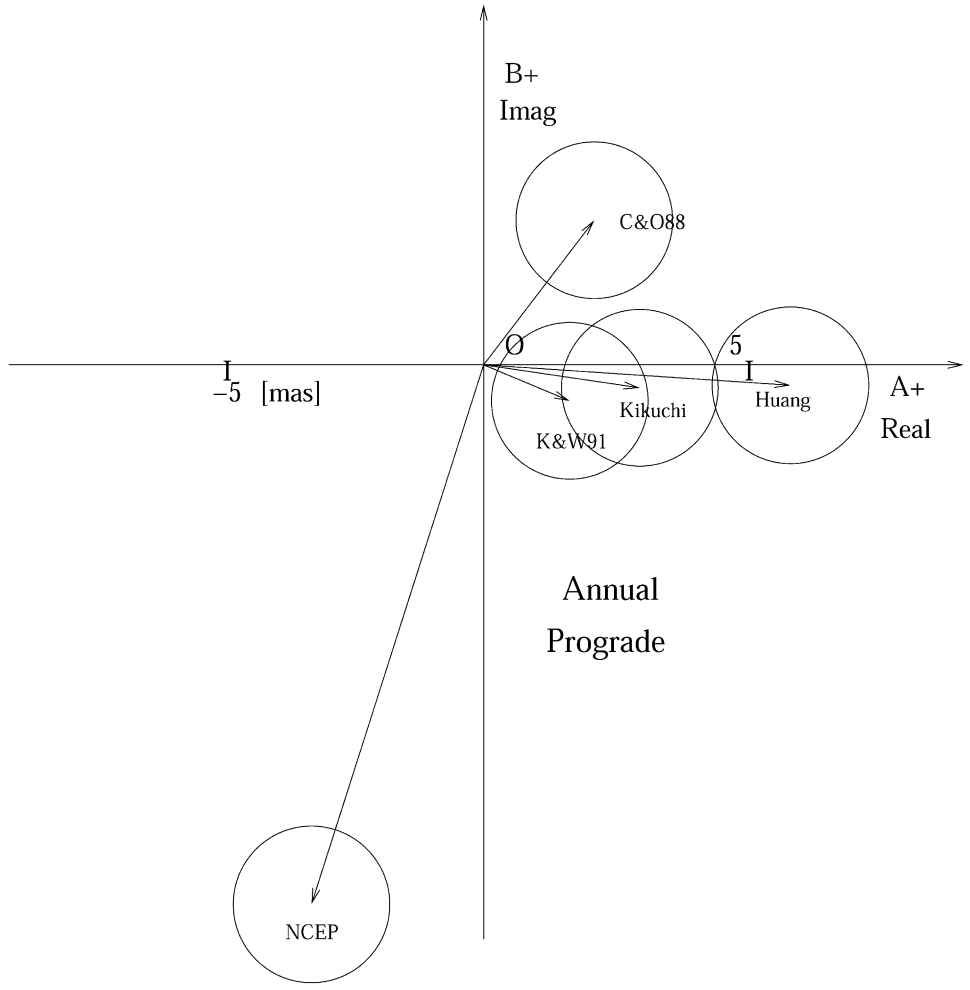

Fig. 2. Phasor plot for the annual prograde component of the excitation function for several models of soil moisture on a plane (A_+, B_+). The abbreviations are from Table 2. Error circles with an estimated radius $\sigma = 1.5$ ma s are also plotted.

5.2. Balance with Chao and O'Connor, 1988

Table 3 presents an example of how the various data sets may be combined in different ways to check the equality of their sum with the geodetic excitation function. Here, 'Chao and O'Connor (1988) sum' = rain + snow is added to the Ponte et al. (1998) ocean model prograde and retrograde coefficients, since the coefficients A_+, B_+, A_-, B_- are additive quantities. This sum is very close to the difference IERS–NCEP atmosphere that remains to be explained. The retrograde component in particular is clearly improved by this inclusion. The OMCT IB results for the ocean also help close the required balance. The Chao and O'Connor (1988) data set was derived especially for Earth rotation purposes. The other soil moisture data sets with greater magnitudes of A_+, B_+, A_-, B_- appear less likely to achieve such a balance.

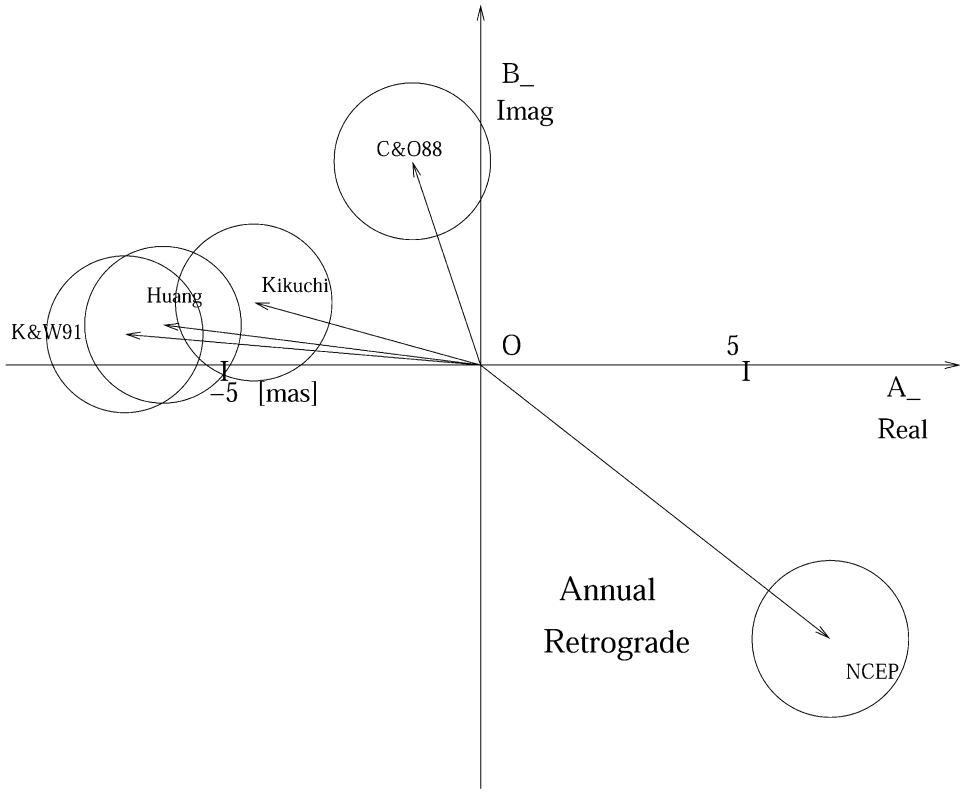

Fig. 3. Phasor plot for the annual retrograde component of the excitation function for several models of soil moisture on a plane (A_-, B_-). The abbreviations are from Table 2. Error circles withan estimated radius $\sigma = 1.5$ ma s are also plotted.

Table 3
Annual balance with Chao and O'Connor, 1988[a]

Description	A_+	B_+	A_-	B_-
Ellipses				
Chao and O'Conner, 1988 sum	0.52	−1.83	2.89	1.60
Ponte et al., 1998 ocean	5.35	4.18	−2.41	6.39
Sum of above	5.87	2.35	0.48	7.99
To be explained				
IERS–NCEP	6.75	4.96	0.44	9.66

[a] Chao and O'Connor (1988) sum = rain + snow is added to the Ponte et al. (1998) oceanmodel prograde and retrograde coefficients, in (ma s). The coefficients A_+, B_+, A_-, B_- are additive quantities.

6. Semi-annual excitation ellipses

We now analyze the semi-annual ($P = 0.50$ a) amplitudes. In Table 4, the new values compared to W2000 are in bold; that is 'OMCT IB' and three soil moisture models. The Inverted Barometer

Table 4
Comparison of semi-annual ellipses of the excitation function χ of polar motion; units are ma s; γ and β are in degrees[a]

Description	A_+	B_+	A_-	B_-	σ_A	a	b	γ	β
Ellipses									
χ From IERS	1.89	6.71	−4.96	2.74		12.64	1.31	112.7	38.4
AAM NCEP smooth	1.91	2.31	−2.04	4.34	±0.66	7.79	−1.79	82.8	32.4
Differences									
IERS–NCEP	−0.02	4.40	−2.92	−1.60		7.73	1.07	149.5	59.2
Hopfner (1996)	−5.00	0.73	−1.21	0.94		6.58	3.52	157.0	345.2
Ocean models									
POCM (CSR)	0.41	0.57	0.39	1.01	±0.04	1.78	−0.38	61.2	7.4
Ponte et al. (1998)	−2.56	0.08	−1.25	−2.05	±1.26	4.97	0.16	28.5	210.2
OMCT (1998)	1.80	−4.87	−4.19	1.93	±1.44	9.80	0.58	42.8	112.5
OMCT IB	0.87	1.37	−0.35	1.33	±1.44	3.00	0.25	81.2	23.7
Soil moisture									
Huang et al. 96 soil	−0.56	1.34	1.11	0.39		2.62	0.27	66.2	313.4
Reanalysis soil (m)	−0.63	335	2.06	−1.74		6.10	0.71	30.1	289.5
Kikuchi calculation	−0.62	0.13	0.69	−0.49		1.49	−0.22	66.5	258.0

[a] 'Reanalysis soil (m).' = model soil moisture from NCEP/NCAR reanalysis (Kalnay et al., 1996), excluding Antarctica.

OMCT run shows a semi-major axis of the excitation ellipse about one third of the earlier model run ['OMCT (1998)', cf. W2000], a positive result since the original was considered too large. Of the three soil moisture models, NCEP/NCAR reanalysis soil moisture has the largest semi-major axis a which may not be realistic. The two other soil moisture modelshave $a \approx 2$ma s and $\gamma \approx 66^\circ$. All three soilmoisture models agree in the quadrant for (A_+, B_+). However, note that the snow load term is still missing here.

7. Conclusions

- The JMA atmosphere gives a smaller residual annual ellipse (observed minus atmosphere) than the NCEP/NCAR reanalysis atmosphere in the cases considered.
- For the ocean alone (without soil moisture) treated by W2000, with phasor plots given in Wünsch (1999),the Ponte et al. (1998) model (MIT model) nearly closes the annual balance, especially in the prograde component. The Hamburg OMCT IB also does quite well, especially the annual retrograde component. The Inverted Barometer assumption has a great influence on the results. Further analysis using improved ocean models needs to be carried out.
- The soil moisture contribution to the excitation function is not yet finally resolved, i.e. the various soil moisture models considered do not agree among themselves. One point of large uncertainty is in the treatment of Greenland, i.e. whether soil or an ice sheet is assumed.
- The snow load contribution is less than or equal to the soil moisture contribution. Better hydrological soil moisture models will become available through the gravity space missions CHAMP (Reigber et al., 2000), GRACE (Tapley and Reigber, 2000) and GOCE (Rummel

et al., 2000). Multiple years of GRACE data would be required for this task. This will lead to new results about the global water cycle.

Acknowledgements

J. Schemm (Climate Prediction Center) gave access to the Huang et al. (1996) soil moisture data set via ftp. M.C. Gennero (GRGS, Toulouse) provided soil moisture coefficients for comparison. H. Jochmann and H. Greiner-Mai (GFZ Potsdam) took part in numerousdiscussions. M. Thomas (University of Hamburg) provided output from the ocean model OMCT. He, L. Ballani and K. Fleming (both at GFZ Potsdam) critically read the manuscript. This work is supported by DFG grant RE 536/7-2.

References

Anon., 1981. Vacuum Cooling for Fruits and Vegetables. Food Processing Industry 1981;12:24.

Abarca del Rio, R., 1997. La rotation de la terre: étude du cycleannuel et de la variabilité basse fréquence. étude climatique de larotation terrestre. PhD thesis, Toulouse.

Aoyama, Y., Naito, I., 2000. Wind contributions to the Earth'sangular momentum budgets in seasonal variation. J. Geophys. Res. 105 (D10), 12417–12431.

Barnes, R.T.H., Hide, R., White, A.A., Wilson, C.A., 1983. Atmospheric angular momentum fluctuations, length-of-day changes and polar motion. Proc. Roy. Soc. London 387 (Ser. A), 31–73.

Chao, B.F., Au, A.Y., 1991. Atmospheric Excitation of the Earth's Annual Wobble: 1980–1988. J. Geophys. Res. 96 (B4), 6577–6582.

Chao, B.F., O'Connor, W.P., 1988. Global surface-water-induced seasonal variations in the Earth's rotation and gravitational field. Geophys. J. 94, 263–270.

Chen, J.L., Wilson, C.R., Chao, B.F., Shum, C.K., Tapley, B.D., 2000. Hydrological and oceanic excitations to polar motion andlength-of-day variation. Geophys. J. Int. 141, 149–156.

Dill, R., 2001. Dissertation in preparation, DGFI Munich.

Gross, R.S., 1992. Correspondence between theory and observations of polar motions. Geophys. J. Int. 109, 162–170.

Gross, R.S., 1993. The effect of ocean tides on the Earth's rotation as predicted by the results of an ocean tide model. Geophys.Res. Lett. 20, 293–296.

Hibler III, W.D., 1979. A dynamic thermodynamic sea ice model. J. Phys. Oceanogr. 9, 815–846.

Höpfner, J., 1996. Polar motion at seasonal frequencies. J. Geodynamics 22, 51–61.

Huang, J., Van den Dool, H.M., Georgakakos, K.P., 1996. Analysis of model-calculated soil moisture over the United States (1931–1993) and applications to long-range temperature forecasts. J. Climate 9, 1350–1362.

IERS, 1997. IERS Annual Report. Central Bureau of IERS, Observatoire de Paris.

Jochmann, H., 1993. Die modifizierte Fourier-Analyse einer zweidimensionalen Bewegung. Zeitschrift für Vermessungswesen 118, 6–10.

Jochmann, H., 1999. The influence of continental water storage on the annual wobble of polar motion, estimated by inverse solution. J. Geodynamics 27, 147–160.

Jochmann, H., Felsmann, E., 2001. Evidence and cause of climatecycles in polar motion. J. Geodesy 74, 711-719.

Johnson, T.J., Wilson, C.R., Chao, B.F., 1999. Oceanic angularmomentum variability estimated from the Parallel Ocean ClimateModel, 1988–1998. J. Geophys. Res. 104 (B11), 25183–25195.

Kalnay, E.etmult.al., 1996. The NCEP/NCAR 40-year reanalysis project. Bull. Amer. Meteorol. Soc. 77, 437–471.

King, N.E., Agnew, D.C., 1991. How large is the retrograde annual wobble? Geophys. Res. Lett. 18, 1735–1738.

Kikuchi, N., 1977. Polar wobble excitation expected from the world precipitation. J. Geod. Soc. Japan 23, 110–118.

Kuehne, J., Wilson, C.R., 1991. Terrestrial water storageand polar motion. J. Geophys. Res. 96 (B3), 4337–4345.

Lambeck, K., 1980. The Earth's variable rotation. Cambridge University Press, Cambridge.
Munk, W.H., MacDonald, G.J.F., 1960. The rotation of the Earth. Cambridge University Press, Cambridge.
Ponte, R.M., Stammer, D., Marshall, J., 1998. Oceanic signals inobserved motions of the Earth's pole of rotation. Nature 391, 476–479.
Ponte, R.M., Stammer, D., 1999. Role of ocean currents and bottompressure variability on seasonal polar motion. J. Geophys. Res. 104 (C10), 23393–23409.
Reigber, Ch., Lühr, H., Schwintzer, P., 2000. Status of theCHAMP mission. In: Rummel, R., Drewes, H., Bosch, W., Hornik, H. (Eds.), Towards an integrated global geodeticobserving system (IGGOS). AG Symp. 120. Springer-Verlag, pp. 63–65.
Robock, A., Schlosser, C.A., Vinnikov, K.Y., Speranskaya, N.A., Entin, J.K., Qiu, S., 1998. Evaluation of the AMIP soil moisturesimulations. Global and Planetary Change 19, 181–208.
Robock, A., Vinnikov, K.Y., Srinivasan, G., Entin, J.K., Hollinger, S.E., Speranskaya, N.A., Liu, S., Namkhai, A., 2000. The Global Soil Moisture Data Bank. Bull. Amer. Meteorol. Soc. 81, 1281–1299.
Rummel, R., Müller, J., Oberndorfer, H., Sneeuw, N., 2000. Satellite gravity gradiometry with GOCE. In: Rummel, R., Drewes, H., Bosch, W., Hornik, H. (Eds.), Towards an integrated global geodeticobserving system (IGGOS). IAG Symp. 120. , pp. 66–72.
Salstein, D.A., Rosen, R.D., 1997. Global momentum and energysignals from reanalysis systems. Preprints, 7th Conf. on ClimateVariations, American Meteorological Society, Boston, MA, 344-348.
Semtner, A.J., Chervin, R.M., 1992. Ocean circulation from a global eddy-resolving model. J. Geophys. Res. 97, C4, 5493-5550.
Stammer, D., Tokmakian, R., Semtner, A., Wunsch, C., 1996. How well does a1/4 degree global circulation model (POCM) simulate large-scale oceanicobservations?. J. Geophys. Res. 101, C10, 25779-25811.
Tapley, B.D., Reigber, C., 2000. The GRACE Mission: Status and Future Plans.Supplement to EOS Transactions of the American Geophysical Union, 81,No. 48, p. F307.
Thomas, M., Sündermann, J., 1998. Zur simultanen Modellierungvon allgemeiner Zirkulation und Gezeiten im Ozean und Auswirkungen aufbestimmte Erdrotationsparameter. In: Freeden, W. (Ed.), Progress inGeodetic Science. Aachen, pp. 144–151.
Thomas, M., Sündermann, J., 2000. Numerical simulations ofocean induced variations of Earth's rotation. In: Soffel, M., Capitaine, N. (Eds.), Proceedings Journées 1999 & IX. , pp. 167–169.
Thomas, M., Sündermann, J., Maier-Reimer, E., 2001. Considerationof ocean tides in an OGCM and impacts on subseasonal to decadal polarmotion excitation. Geophys. Res. Lett. 28, 2457–2460.
Wahr, J.M., 1982. The effects of the atmosphere and oceans on the Earth's wobble– I. Theory. Geophys. J. R. astr. Soc. 70, 349–372.
Wahr, J.M., 1983. The effects of the atmosphere and oceans on the Earth'swobble and on the seasonal variations in the length of day–II. Results. Geophys. J. R. astr. Soc. 74, 451–487.
Wünsch, J., 1999. Oceanic influence on the seasonal polar motion.GFZ Potsdam Scientific Technical Report STR 99/10.
Wünsch, J., 2000. Oceanic influence on the annual polarmotion. J. Geodynamics 30, 389–399.
Wünsch, J., Thomas, M., Gruber, T., in press. Simulation of oceanicbottom pressure for gravity space missions. Accepted by GJI.